Automatic Characterization of the Cell Organization in Light Microscopic Images of Wood: Application to the Identification of the Cell File

Guilhem Brunel[1,2], Philippe Borianne[2], Gérard Subsol[3], Marc Jaeger[2] & Yves Caraglio[2]

[1]UMII; [2]CIRAD – UMR AMAP
Montpellier, France
Guilhem.brunel@cirad.fr

[3]CNRS – LIRMM
Montpellier, France

***Abstract* — Automated analysis of wood anatomical sections is of great interest in understanding the growth and development of plants. In this paper, we propose a novel method to characterize the cell organization in light microscopic wood section images. It aims to identify automatically the cell file in a context of mass treatment. The originality of the proposed method is our cell classification process. Unlike many supervised methods, our method is self conditioned, based on a decision tree which thresholds are automatically evaluated according to specific biological characteristics of each image. In order to evaluate the performances of the proposed system and allow the certification of the cell line detection, we introduced indices of quality characterizing the accuracy of results and parameters of these results. Those are related to topological and geometrical characters of the cell file at both global and local scales. Moreover, we propose an index of certainty for selective results exploitation in further statistical studies. The proposed method was is implemented as a plugin for ImageJ. Tests hold on various wood section well contrasted images show good results in terms of cell file detection and process speed.**

Keywords: Image processing, pattern recognition, wood microscopic images, cell segmentation, file identification.

I. INTRODUCTION

The development of the tree results from the primary growth and secondary growth. The primary growth concerns the extension and branching of the axes. Whereas the secondary growth is on their thickening. Among others, issues of carbon squestration and wood energy leads to consider both structural and functional aspects using acumulating approaches. Howhever, these approaches, concerning secondary growth and its relationships between secondary and primary growth, are based on fragmentary studies, mainly raising from data acquisition costs. Secondary growth results from the cambial activity, which is among other things to the origin of wood (xylem) and consequently the different cellular elements that constitute it. The understanding of mechanisms of growth of the cambium will go through the study of rhythmicity of cell patterns, their disruption or modification through space and time. Environment and its fluctuations influence the differentiation of wood's elements (from the divisions of cambial cells) which constrain us to follow the production of specific cell organizations. To simplify, two organizations are considered: firstly the growth rings which represents cell's production at a given time [1], and secondly the cell lines which represents the activity of an initial cell during time [2]. For example, [3] underlie the importance of secondary growth organizations by studing cellular patterns, their spatial rhythmicity, their variability along different growth rings. For its part, the study of cell lines is presented as a promising enable to understand the development, differentiation and temporal rhythmicity of cells [4]. Automating the study of cell lines should permit to closer links with the functional aspects and ecology of species: Wood is a continuous recording of changes in the development of the tree (the lesser known) and its environment (the most work, eg dendrochronology, tree-rings).

Progress in terms of the image acquisition devices and their analysis allow us to consider the access to quality's information on various extensive areas in the plant. Cross section microscopic images analysis shows interest in both cell feature characterization and detection but also for higher structure character estimation as shown for instance by Wu et al on root sections [5].

Automatic identification of wood cellular structures as cell files is a new challenge in structural biology of plants [6], which requires a multidisciplinary expertise.

In bio-imaging, cell segmentation has been intensively studied by researchers in image processing with various approaches [7][8][9]. For example, [10] combine four classical algorithms to segment white blood cells in bone marrow image: watershed [11], snake [12], multi-resolution analysis [13] and dynamic programming. This kind of approach based on mixing many algorithms, shows the difficulty of segmenting cell images with high biological variability. The algorythms should be adapted to the application and to the specific cells characters. In particular, for wood cross section, we have to consider both cell local geometry and arrangement.

In such wood cellular organizations, some authors propose to introduce some geometric models to describe the topological neighborhood of cells. For example, [14] or [15] rely on an oriented graph to extract cell files in images of the gymnosperms.

From a technical point of view, we did not found any software solution allowing automatic identification of cell files. Some specific commercial tools as WinCell [23], exist for the analysis of wood cells, but they do not allow recognition and characterization of the cellular organization. Moreover, it is not possible to add new functionalities. More

978-1-4673-0070-4/12/$31.00 ©2012 IEEE

generic commercial software such as Visilog [24], offer a rich development environment in image processing but they are quite expensive and not sufficiently specialized for our application. Open source platforms as ImageJ [20][25] are an attractive option: they allow to enrich the source code with specific functionalities while facilitating the exchange and dissemination of methods. Therefore we chose this solution to implement our algorithm.

The proposed method of automatic identification and modeling of cell files extends the research presented by [15]. In this work, cell file identification in light microscopy images is based on a preliminary identification of the cells. It is a supervised classification requiring the definition, then the use of a large training database. As the variability of wood anatomy is huge, significant results can be obtained only for a limited number of wood species, sharing close and simple anatomical features (gymnosperms in this case). We introduce here a specific model of the cell lines recognition avoiding supervised training and allowing results quality quantification. Applying this model, as shown in the following sections, we can build a generic tool suitable for both gymniosperm and angiosperm wood cross section images.

II. MATERIAL AND METHOD

A. *Preparation and digitization*

We aim to process histological stained sections of angiosperm and gymnosperm wood, and more specifically of Mahogany, Fraxinus Angustifolia, Pine Black, Pine Carabinsis and Fir tree.

Wood cross sections of 20-25 µm of thickness are produced with a vibratome. They are then immersed in an aqueous chlorinated solution to clean the cellular content. A colouring of the cell wall is then performed to increase the contrast with the lumen. Various types of colouring agents can be used as the methylene blue, the toluidine blue or the safranine. The sections are then digitized by a Olympus DP71 LCD camera mounted on a Olympus BX51 microscope. The magnification is choosen around ×100.

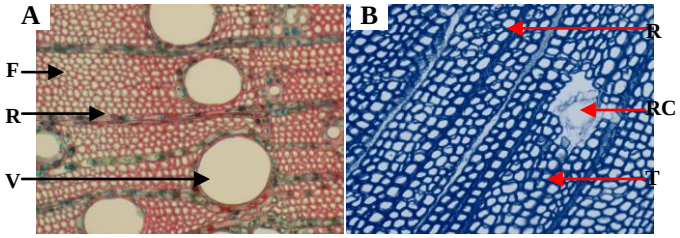

Figure 1. Images of histological stained wood sections. A: Fraxinus (angiosperm) colored with safranin. B: Pinus Caribensis (gymnosperm) colored with methylene blue. Notice the different anatomical structures: Vessel (V), Ray (R), Fiber (F), Tracheid (T) and Resin Canal (RC).

Different anatomical structures as vessels, fibers, tracheids, resin canals, or rays are visible around the cell files (see Fig. 1). With such a magnification value, we can count at least 20 consecutive cells and then distinguish the cell files and the smallest interesting structure covers a surface of at least 10 by 10 pixels.

The resulting images are in color (coded on 24 bits) with a resolution close to 2000 by 2000 pixels.

B. *Cell file processing*

Identification of cell files is based on the search of alignment of cells which share similar geometric (i.e. size, shape) and densitometric (i.e. color) properties. The concept of alignment implies a specific cellular organization which is emphasized by the neighborhood relations between cells.

Our approach is divided into three steps (see Fig. 2): first cell identification is performed in order to individualize the cells in the image, then the cellular organization step detects and individualizes the alignments of anatomical structures, and finally, the classification step classifies anatomically and types qualitatively the cell files. In the following sections, we detail these three steps.

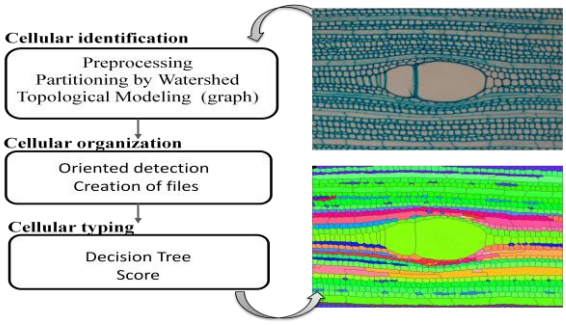

Figure 2. Overview of the cell file identification algorithm.

1) *Cell identification step*

Microscope images present a "pepper-and-salt" noise inferred by the thermal effect of the lamp. We attenuate this impulsive noise by applying a median filter of radius 3 pixels. Images show alternations of clear and dark areas representing respecitvely the cell lumens and the cell walls. To increase the contrast between the two areas, we apply the Difference of Gaussian (DoG) [16] method. This is a bandpass filter. It thresholds the frequencies corresponding to the lumens. To obtain the lumens (see Fig. 3), the DoG filter subtracts a Gaussian light blurred image (blurring parameter close to the size of the cell wall) to the highly blurred image (blurring parameter set to 1/10 of the image width). Nota that the blurring parameters were set experimentally and are different from the classical 1.6 ratio used for DoG smoothing in edge detection.

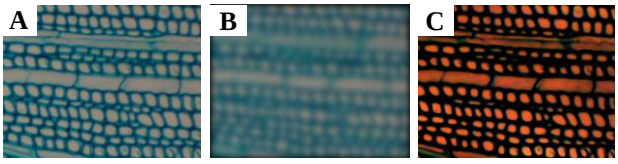

Figure 3. Difference of Gaussian filtering on a cross-section of Mahogany stained with toluidine blue. A: the image obtained by applying a small Gaussian blurring (σ = 3 pixels). B: the image resulting from a strong Gaussian blurring (σ = (image width)/10). C: subtraction of images A and B which increases the contrast wall / lumen.

We obtain an image where the walls have zero intensity and the lumens have a higher intensity.

This colour image is then converted in grey levels. Average colour channel value is used since no specific channel seems significant. Moreover this conversion simplifies specific process definition potentially resulting from different colouring protocols.

The greyscale image cell extraction is obtained by the classical Watershed algorithm [11]. The idea is to consider a grey level image as a topographic relief, and to calculate the watershed lines by "flooding" the relief. The resulting watershed lines define a partition of the image. The ridge lines constitute the intercellular boundaries and correspond to the middle lamella. The lines of the ridges of the Wathersed (fig. 4-c) give the boundary between two adjacent watersheds. The dual graph is the adjacency graph of the basins, it connects two by two the geometric centers of the basins incident to the same edge. The basins are superimposable to image cells, we speak of the adjacency graph of the cells (Fig. 4-d).

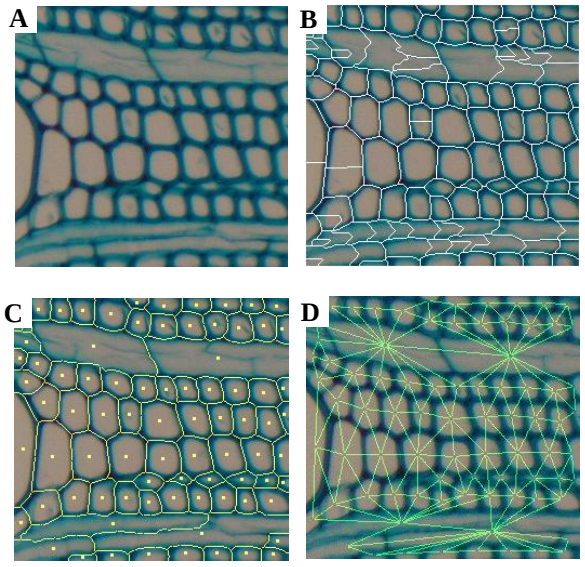

Figure 4. Cell individualization of a Mahogany cross section. A: native image. B: watershed segmentation result with the crest lines crossing the lumen. C: cleaned watershed: the crest lines are replaced by curvilinear edges shown in yellow; they correspond to the middle lamella; the points extra yellow match the geometric center of the watershed therefore biological cells. D: dual watershed graph. This adjacency graph, in green connects cell centers with their neighbour; notice that the degree of vertices is greater than four showing the staggered pattern of the cells.

2) Cellular Organization

Unlike approaches [15] and [14], our recognition of lines based exclusively on a constraint path of the adjacency graph of the cells. More specifically, the construction of cell lines is based on the one hand on geometric criteria, in particular the general orientation of adjacencies cell, and, secondly on topological criteria, in particular on configurations of cellular adjacency.

The edges of the adjacency graph represent connections between neighboring cells and their orientations give an indication of the preferred directions of the cell arrangements. On our studies, cells are arranged in staggered rows, and cell lines are rectilinear and two in two parallels. Therefore, the orientations of edges adjacency follow three directions: a main one, corresponding to the cell alignments and two secondaries, corresponding to the organization in staggered rows (fig. 4-d). To compute the main direction, we use R. Jones (1996) method, studying the distribution of angles formed by each edge of the adjacency graph with the horizontal. The distribution is then trimodal : the major mode shows the orientation most present in the adjacency graph, that is to say the general orientation of the lines (Fig. 5).

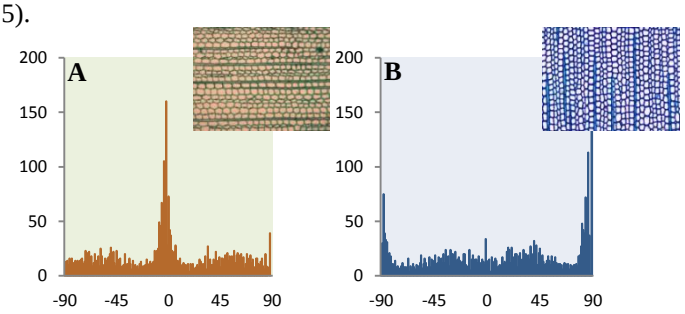

Figure 5. Direction distribution histograms formed by edges of the adjacency graph with the horizontal. A: The main mode centered on 0° corresponds to horizontal lines; B: The histogram shows one mode splitted on -90 and 90° values corresponding to vertical lines.

Considering now the lines. The construction is progressive and based on four principles: alignment search, feedback check, overlap management and chaining. The alignment principle allows for each vertex V of the graph to find the next vertex NV in the cell lines. Each vertex neighbor of V is a potential candidate. We will retain one that maintains the best spatial alignment (in a range of ± 35 °), and whose underlying cell shows the highest geometrical similarities with the previous one. The line is gradually built from the initial edge, by successive additions of consecutive edges preserving the geometric continuity. At each step, the drift of the line is minimized under this geometrical constraint. We chose the criterion of Bray-Curtis [21] (see Fig. 6) for similarity cost evaluation since well adapted to surface characterizations. When this criterion tends to zero, the compared cells can be considered as similar.

$$BC_{nm} = \frac{|n - m|}{(n + m)}$$

Figure 6. Formula of Bray Curtis. Where « n » is the surface of current cell and « m » is the surface of neighbor cell. When the criterion tends to 0, the cells show a similar surface.

Each cell bellowing to a cell line path is given a score value : the sum of the angle deviation with its predecessor and the criterion of Bray-Curtis.

The path of the line stops when there are not vertices anymore candidate.

A cell line direction is independent from graph traversal orientation. This property is used to validate or invalidate any line segment or part of if. The process described above is applied again starting from the end edge, by inverting the direction of progress in the graph. We note this path as "backward", opposed to the initial path "forward". This define the principle of Forward / Backward : a line is validated when both forward and backward paths are strictly superposables. In the case where the paths are not identical, the initial forward path is gradually reduced until reaching a stable forward/backward sub-path. Specifically, whenever a difference appears in backward path, the corresponding segment is deleted from the original line: the edges and their scores are released, initialized to an infinite value. The backward tip is updated from the last reached position. In the strictly superposable case, the score of each cell of the line is decreased by half insuring higth stability of the line towards overlaping (see below).

Indeed, a cell belongs to a unique file. This property leads to the following rule: each vertex belongs to one cell line and only one. In some cases, during its construction, a line may use one or several cells, mobilized by a line already constructed. In this case, each of these vertex is attributed to the line for which its score is minimal: it is the principle of overlaping. Two scenarii may occur:

- The existing line keeps its vertex; the line under construction will have to find another path or stop.
- The existing line loses its summit to the detriment of the line under construction. Here, all the summits of the existing line situated after the lost summit are released: their respective score takes an infinite value, indicating they are again available.

Due to the presence of intrusions, tearings or a lack of adjency (Fig. 7-a), it is not unusual to detect a given line in splitted part.

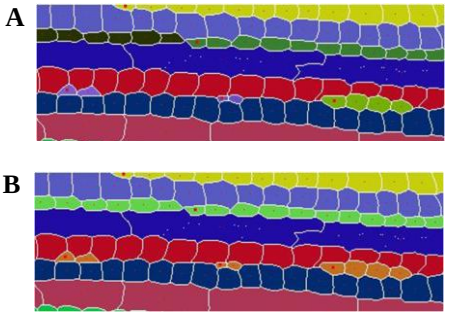

Figure 7. A: Result of treatment chain without connection. B: result whit connection (Bottom). There is one color by file.

The principle of merging allows to concatenate several part of line, using simple topological rules, to establish whole lines. The idea is based on two observations : (i) the lines cross the image throughout, (ii) the lines do not intersect (Fig. 8-a). As a result, if the parts T2 and T2 ' are adjacent to the line F1 and F3, it is likely that T2 and T2 ' are two parts of the same line F2. At present only the parts in two same lines are concatenate that is to say as belonging to the same line. In other scenarii the process is stopped.

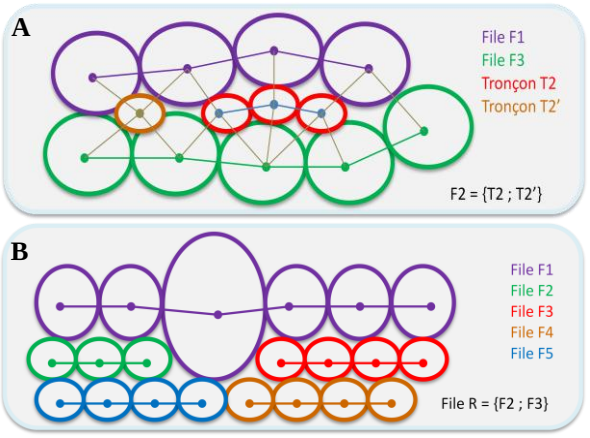

Figure 8. A: a two neighbours connection scheme. Sections T2 and T2' are squeezed between lines F1 and F3; therefore T2 and T2' are probably derived from a common file F2. B: a multiple neighbours scheme; in this case, rules of adjency are used to drop the case in a two neighbours one.

3) Classification step

The cell typing is the ultimate step: it allows to classify different cells (fibers, tracheids, vessels, rays, ...). It is realized from geometric and densitometric characterization of the watersheds associated with the vertices of the adjacency graph of cells. Unlike the work of [15] and [14], supervised classification was discarded because of the difficulty of building learning games sufficiently complete and discriminating, due to the existing biological variability.

A decision tree discriminates the anatomical structures. It was established with wood anatomists from the two following hypotheses:

1) The perimeter of cells, noted parameter T, allows to differentiate the "big" structures from the "small" cells.

2) The circularity of cells, noted parameter C, allows to differentiate rays (globally lengthened) from the vessels (globally circular).

The decision tree given in Fig. 9 is applied to basins with a clear area corresponding to the lumen. It requests two threshold values which are automatically estimated for every image. For each parameter, both values are calculated from the grey image, from two disjoint groups using a two-means clustering [22]. This classical method divides n observations into two clusters, so minimizes the intra-classe variance and maximizes the interclasse variance. The threshold is then given by the median value between the upper bound of the lowest group and the lower bound of the stronger group.

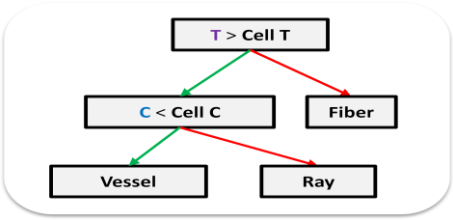

Figure 9. Decision Tree. T represents the threshold of the perimeter and C the threshold of circularity. The thresholds are automatically rated by a 2-means clustering applied to all values from the image. Only cells with a lumen are processed by the decision tree.

After the alignments identification and the biological typing, we can deliver a set of figures characterizing the shape, size, nature of biological structures (walls, lights, cells, lines ...). These characteristics, of interest for anatomists, are defined by self conditioned procedures. As part of a mass treatment it is interesting to characterize the accuracy of these assessments. Both caracteristic quality and automated define parameters are computed defining indexes of certainty. An index is assigned for each calculated parameter. The certainty index concerns the geometric parameters of structural elements and the steps of the process of identifying lines.

At the scale of structural elements (fiber, vessels, radius ...), evaluation of this index depends on the parameter itself. For example, the certainty of the surface or the shape of the lumen is directly connected to the local degree of sharpness of the image (Fig. 14): the boundary between the wall and the lumen being obtained by distribution of the pixels of the cell two intensity classes (light intensities and dark intensities), it depends irremediably on local dynamics of the image.

At scale structure elements (lines), evaluation of the index depends on the construction process and the nature of the result. To "certify" the cell lines, three criteria are used :

- The overall score of the line, characterizing topological relationships of the line with its neighbors. The identification of the topological position allows to assign a global additional score to the line: 0 for a line crossing the image throughout, 1 for a line composed of simple parts, 2 for non indentified segment, 3 for single cell, 4 for defects.
- The average of the scores of its cells obtained during the construction of the line (not to be confused with the index of certainty parameters). Each vertex added to the line will be assigned a score defined by the sum of the deviation of the angular aperture and the similarity coefficient. This method allows to restrict the path of the line without guaranteeing possible overlapping or intersection with a nearby line.
- The length, characterizing the representativeness in the image: the more a line is long, the more it is sure.

An index of certainty is assigned to the line according a linear combinaison of these three scores. The indices of certainties (parameters and lines) are used to filter or classify the numerical results generated for each lines identified.

The indices of certainty of the lines are totally independent from indices certainties of the parameters associated with the cells.

The visual representation of the global score of the lines, and in particular the use of a color code, allows a fast and efficient processing check, distinguishing the whole lines form the cellular insertions. The colour code is green for the lines automatically identified, is blue for lines automatically rebuilt and is red for complex configurations (Fig. 10).

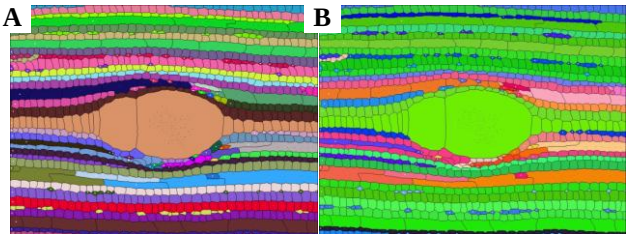

Figure 10. Automatic identification of cell lines from a cross section of mahogany. A: lines random colouring is used. B: colour qualifies the cell files; the lines automatically identified in green, the lines automatically rebuilt in blue and the complex configurations in red.

The method has been implemented in Java and integrated as a plugin in the ImageJ free platform. We use additional free libraries sush as the Java Universal Network / Graph Framework [26] for efficient data structure management. We are currently posting the application on the web [27].

III. RESULTS AND DISCUSSION

The tests were led from a sample of images representative of biological variability, possessing a dozen colored sections of different species of angiosperms (list) and gymnosperms (list) (Fig. 11).

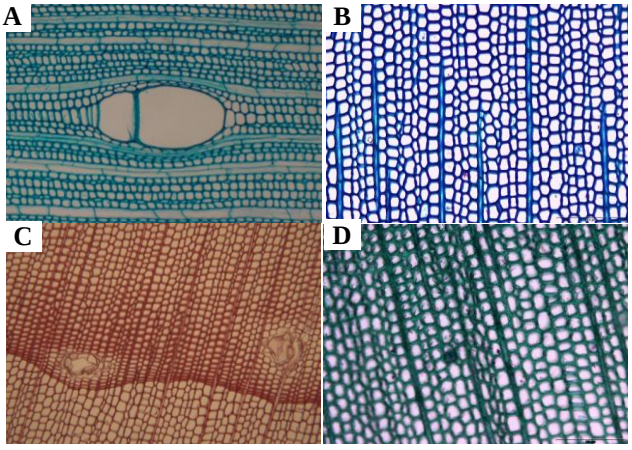

Figure 11. Extract from the test set consists of cross sections of angiosperms and gymnosperms. A : mahogany colored with toluidine blue for which the continuity of queues is preserved in spite of the vessel elements. B : fir colored with methylene blue. C : black pine colored with safranin having resin canals. D : fir colored with toluidine blue showing cells blocked.

A. *Biological aspecsts*

Moreover, the colour encoding can quickly locate the complex biological configurations requiring the expertise of an anatomist to be identified (in red, Fig. 12).

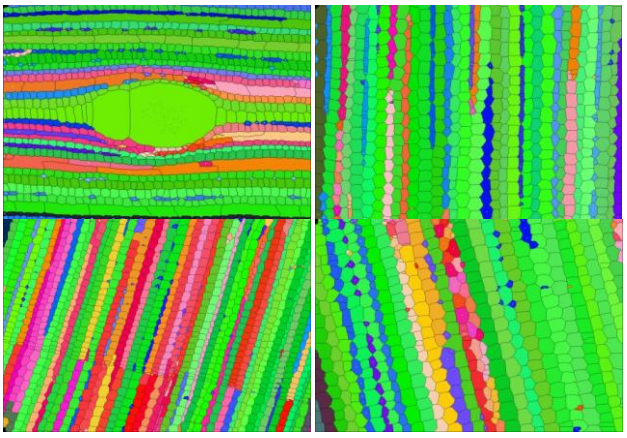

Figure 12. Automatic identification of cell lines of the extract on the game of trying to figure 11. The colour code is given in figure 10.

As shown in the table below, our method works well on images presenting a structured organization with a marked wall / lumen contrast, in regard to data acquisition, management of lines and the magnification used. For configurations showing low colour contrast or complex cellular organizations the lines are badly detected.

Table 1. Summary of some significant results: the size of images processed, the number of cells extracted, the CPU time obtained on a machine with an Intel Xeon at 2.3GHz and a Total Quality Index defined as the ratio of the number of lines automatically identified and reconstructed on the total number of lines.

Species	Size (pixels)	Cells numbers	Times (sec)	Total Quality (%)
Mahogany	1024x768	1359	14.3	83
Fir	1360x1024	800	12.4	92
Black Pine 1	1600x1200	1873	23.2	73
Caribean Pine	1360x1024	828	11.5	91
Black Pine 2	1600x1200	1458	16.1	93

What about in terms of quantity, that is to say in terms of numerical measures?

The overall rating of the line remains the most important indicator. It enables us in particular to detect all single files: all lines described as obvious by anatomists have an overall zero score.

On the test set, the lines are automatically detected at 60% in the images. This figure is not significant since it depends on the anatomical configurations. The unidentified lines can be automatically excluded from statistical processing. The amount lost can be easily offset by the increase of the images treatable.

It is important to evaluate the accuracy of measurement. The Figure 13 presents the comparison of about sixty normalized aeras got from manual and automated method. The coefficient of determination tends of 1 showing the areas are well correlated. The slope of regression line is weakly superior to 1 indicating a weak over-valuation of the automated method. The weak gap of 0.0127 confirms the middle error of 5% on right areas. The automated method seems over-valuated the measurements (at least the expert under-valuates the measures!). Only certainty: the automated method is repeatable.

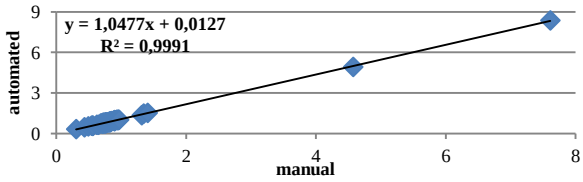

Figure 13. Basins surfaces study on Mahogany. In abcissa, the normalized aeras got from the fully manual method. In ordinate, those got from the automated method. The coefficient of determination is close to 1, showing a very well adjustment of areas.

The major limit to the automatic identification of lines comes from the image content, that is to say the photometric characteristics of the image, and biological configurations.

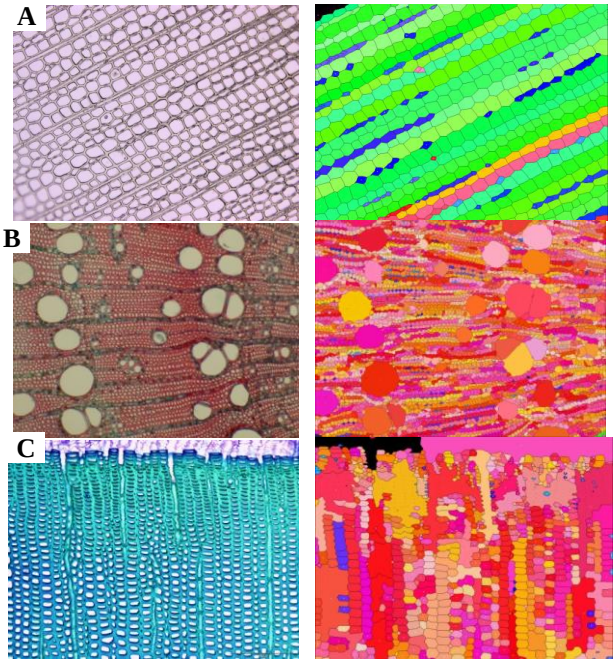

Figure 14. A right cross sections of three native species. On the left, the automatic identification of cell lines. A : not colored pine treated in transmission; Detection is good despite the low constrate Wall / Lumen. B : ash colored with safranin; Detection of cells is good, but the method only produces sections due to the complexity of biological organization. C : pine colored with methylene blue; Identification is biased by the presence of local inversion of contrast at the joinction wood summer / winter.

The images with a dynamic intensity locally reversed, for example the junction wood winter / summer wood (Fig. 14-c), remain difficult to treat. Our method is based on the image contrast, so watersheds corresponding to the cells are badly detected, and thus the detection of files is incorrect

and incomplete. The images of washer sanded wood (unstained) are treated in reflection: light does not pass through the sample. Thus the lumens appear in colour almost close to the walls one, with not sufficient contrast to ensure proper recognition of watersheds and proper identification of lines. The wood sections not colored are treated by transmission, crossed by light. They are less contrasted than the stained sections. But the difference wall / lumen is pronounced enough to allow the algorithm to correctly identify the lines (Fig. 14-a). For complex cellular organizations (Fig. 14-b), where cell alignments are not obvious, new rules for the path and for the reconstruction shloud be established with the biologists.

The files are created using only geometric and topological rules on the basins. It is important to make sure of the robustness of the detection of the basins, expecially internes of insensitivity to blur and image orientation. A first study was conducted on the absorption of the blur found in images related to microsope views side effect or sample flatness.

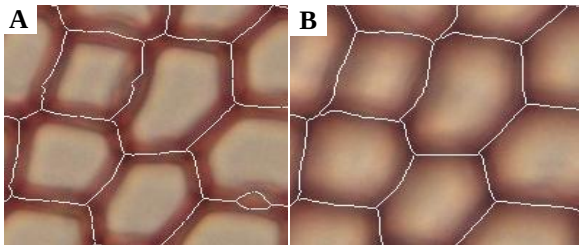

Figure 15. Compared watershed result on Pine cross section. A : crests lines of a sharp image. B : crests lines of a blurred image. Outline of the basins is nearly identical between a sharp and a blur image. On the sharp image, a small additional basin of a detachment of the wall issued from cutting. This basin is skipped during the supernumerary removal phase.

Acquisitions of the same zone of the image with different focus were performed to evaluate the stability of our computational method. In particular, we made a statistical study on the variability of cropping cells. The intercellular lines obtained by the algorithm of Watershed are generally invariant to blurring of the image. Indeed, they correspond to the curves reverse slopes of intensity: the smoothing of the image produced by optical blur attenuates the intensity without changing the look of intensity variations. The crest lines remain unchanged (Fig. 15).

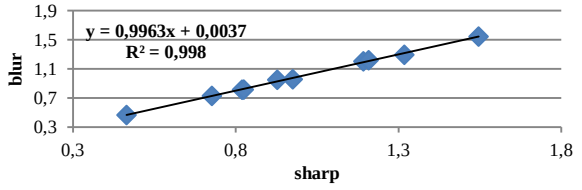

Figure 16. Basins surfaces study on Mahogany. In abcissa, the normalized aeras got from sharp images. In ordinate, those got from blur images. The coefficient of determination is close to 1, showing a very well adjustment of areas.

Figure 16 shows the comparison of a sixty normalized area obtained from a sharp and a blurred image. The coefficient of determination tends to 1 showing areas are well correlated. The slope of the regression line is slightly less than 1 indicating low undervaluation on blurred images. The difference of 0.0037 confirms the average error of 2.81% on sharp image. The method gives results almost identical regardless of the sharpness of the image

The method described is working correctly for images that contain the one hand high contrast between the walls and lumens (without local inversion of color) and other hand a visible cellular organization. Under these conditions all the obvious lines by qualified experts are correctly identified, with a significant time save (a typical manual expert identification requires ten hours on our samples). Moreover, the index of certainty allows the selective exploitation of results for statistical studies.

IV. Conclusions

Automated analysis of wood anatomical sections is of great interest in understanding the growth and development of plants. In a frame of over studies on wood structure, we propose a original method for automatic detection of cell lines, operational in mass treatment. It applies to digital images of coloured transverse cut wood. Identification of lines based on research alignment of cells presenting similar geometrical and densitometric characteristics. The notion of alignment implies to know how to set up the relations of neighborhood between cells. Identification of lines is made from an adjacency graph for the path constrained graph with an orientation and similarity criteria. The originality of the method compared to a supervised method is that it automatically creates rules evaluated for each image and not a set of rules to be applied on all images. The lines described as obvious by anatomists are correctly identified by our method, with a drastic drop of time cost. To "certify" the cell lines, we have introduced the indices characterizing the quality of results and parameters of these results. The method described works correctly for images with high contrast between the walls and lumens and a clear cellular organization. Under these conditions all the obvious lines by qualified experts are correctly identified. Moreover, the index of certainty allows the selective exploitation of results for statistical studies.

Three future work axes are being considered:

1. The enlargement of the major zones of study in order to follow the lines of several rings (Fig. 17). For this, it is necessary to adapt the processing of image mosaics. Two problems are directly related: first, the treatment of different photometric behavior in the same image, in particular the transition wood winter / summer wood. Secondly, the joining of the results at the edges of the images pavement.
2. The study can be extended to sanded wood, for which the contrast wall / lumen is less contrasted.
3. The enrichment of the cell typing method that is not currently able to differentiate all kind of vessels. Work

on the walls texture can be considered to resolve the limitation.

Cell file identification has to deal with other open difficulties like the passage tree ring or the junction between the different images. The construction of cell lines will be reviewed to match between images that may or may not be recovered.

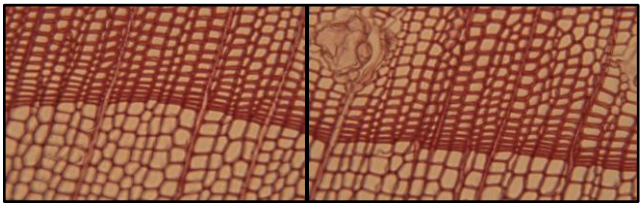

Figure 17. Abutting mosaic of a cross section of Black Pine, colored with safranin, 100x.

As a summary, this work is a first contribution to develop methods for automatic image processing that will mainly to identify and characterize, in mosaics depicting field's broad observation, cellular organizations, and the cells that compose them. The implementation aims to obtain a rapid cell typing, automatic and reliable to process statistically significantly large sets of data.

ACKNOWLEDGMENT

The authors gratefully acknowledge Christine HEINZ for her involvement in this work, her advices and availability. A big thank to Michael GUEROULT without whom the laboratory work would not have been possible.

This work is jointly funded by a doctoral fellowship of the Labex NUMEV and the SIBAGHE Graduate School of the University Montpellier 2 and by the Scientific Council of the University Montpellier 2.

REFERENCES

[1] L. Heinrich, "Reaction wood varieties caused by different experimental treatments," TRACE, Tree Rings in Archaeology, Climatology and Ecology, vol. 5, p. 224–232, 2007.

[2] P. Rozenberg, G. Schüte, M. Ivkovich, C. Bastien, and J.-C. Bastien, "Clonal variation of indirect cambium reaction to within-growing season temperature changes in Douglas-fir," Forestry, vol. 77, no. 4, pp. 257 –268, Jan. 2004..

[3] E. Nicolini, Y. Caraglio, R. Pélissier, C. Leroy, and J. Roggy, "Epicormic Branches: a Growth Indicator for the Tropical Forest Tree, Dicorynia guianensis Amshoff (Caesalpiniaceae)," Annals of Botany, vol. 92, no. 1, pp. 97 – 105, Jul. 2003..

[4] W. Gindl, "Cell-wall lignin content related to tracheid dimensions in drought-sensitive austrian pine (pinus nigra)," Iawa Journal, vol. 22, no. 2, pp. 113–120, 2001..

[5] Haiwen Wu, Marc Jaeger, Mao Wang, Baoguo Li and Baogui Zhang. 3D-Reconstruction and Visualization of Xylem Vessels of Wheat Nodal Root. In: Li, B. and Jaeger, M. and Guo, Y. (Eds). 2010. Proceedings,of Plant growth Modeling, and their Applications (PMA09), Beijing,,China, November 9-13, 2009, IEEE CPS, pp. 384-390

[6] P. Quelhas, J. Nieuwland, W. Dewitte, A. M. Mendonça, J. Murray, and A. Campilho, "Arabidopsis Thaliana Automatic Cell File Detection and Cell Length Estimation," in Image Analysis and Recognition, vol. 6754, M. Kamel and A. Campilho, Eds. Berlin, Heidelberg: Springer Berlin Heidelberg, 2011, pp. 1–11.

[7] M. K. Moëll and L. A. Donaldson, "Comparison of segmentation method for digital image analysis of confocal microscope images to measaure tracheid cell dimensions," IAWA Journal. Vol. 22(3), pp. 267–288, 2001.

[8] D. Baggett, M. Nakaya, M. McAuliffe, T. P. Yamaguchi, and S. Lockett, "Whole cell segmentation in solid tissue sections," Cytometry A, vol. 67, no. 2, pp. 137–143, Oct. 2005.

[9] T. Fourcaud, X. Zhang, A. Stokes, H. Lambers, and C. Körner, "Plant Growth Modelling and Applications: The Increasing Importance of Plant Architecture in Growth Models," Ann Bot (Lond), vol. 101, no. 8, pp. 1053–1063, May 2008.

[10] J. Park and J. M. Keller, "Snakes on the Watershed.," IEEE Trans. Pattern Anal. Mach. Intell., pp. 1201–1205, 2001.

[11] L. Vincent and P. Soille, "Watersheds in Digital Spaces: An Efficient Algorithm Based on Immersion Simulations," IEEE Transactions on Pattern Analysis and Machine Intelligence, vol. 13, no. 6, pp. 583–598, Jun. 1991.

[12] Kass, A. Witkin, and D. Terzopoulos, "Snakes: Active contour models," Int J Comput Vis, vol. 1, no. 4, pp. 321–331, 1988.

[13] M. B. Jeacocke and B. C. Lovell, "A multi-resolution algorithm for cytological image segmentation," in Proceedings of the 1994 Second Australian and New Zealand Conference on Intelligent Information Systems,1994, 1994, pp. 322–326.

[14] R. Jones and L. Bischof, "A graph–based segmentation of wood micrographs," in Computing Science and Statistics, 28, Sydney, 1996, pp. 12–20.

[15] P. Kennel, G. Subsol, M. Guéroult, and P. Borianne, "Automatic identification of cell files in light microscopic images of conifer wood," in 2010 2nd International Conference on Image Processing Theory Tools and Applications (IPTA), 2010, pp. 98–103.

[16] G. T. Einevoll and H. E. Plesser, "Response of the difference-of-Gaussians model to circular drifting-grating patches," Vis. Neurosci., vol. 22, no. 4, pp. 437–446, Aug. 2005.

[17] L. Breiman, J. Friedman, C. J. Stone, and R. A. Olshen, Classification and Regression Trees, 1st ed. Chapman and Hall/CRC, 1984.

[18] O. M. Hitz, H. Gärtner, I. Heinrich, and M. Monbaron, "Wood anatomical changes in roots of European ash (Fraxinus excelsior L.) after exposure," Dendrochronologia, vol. 25, no. 3, pp. 145–152, Mar. 2008.

[19] A. J. Travis, D. J. Hirst, and A. Chesson, "Automatic Classification of Plant Cells According to Tissue Type using Anatomical Features Obtained by the Distance Transform," *Annals of Botany*, vol. 78, no. 3, pp. 325 –331, 1996.

[20] B. Clair, J. Gril, F. Di Renzo, H. Yamamoto, and F. Quignard, "Characterization of a Gel in the Cell Wall To Elucidate the Paradoxical Shrinkage of Tension Wood," Biomacromolecules, vol. 9, no. 2, pp. 494–498, 2007.

[21] J. R. Bray and J. T. Curtis, "An Ordination of the Upland Forest Communities of Southern Wisconsin," Ecological Monographs, vol. 27, p. 325, Oct. 1957.

[22] E. Forgy, "Cluster analysis of multivariate data: efficiency vs interpretability of classifications," Biometrics, vol. 21, pp. 768–769, 1965.

[23] http://www.regentinstruments.com/

[24] http://www.noesisvision.com/fr/index.html

[25] http://rsbweb.nih.gov/ij/index.html

[26] http://jung.sourceforge.net/doc/index.html

[27] http://umramap.cirad.fr/amap2/logiciels_amap/index.php?page=ficeler